EAST EUROPEAN JOURNAL OF PHYSICS. 3. 347-356 (2026)
DOI:10.26565/2312-4334-2026-3-30 ISSN 2312-4334

EFFECT OF PRESSURE ON THE ENERGY BAND STRUCTURE OF AlAs USING sp3s* MODEL

Ali A. Mohammed[1]*, Mumtaz M.S. Hussien[2], Abbas Hussein Rostam[3]*****
[1]*Department of Physics, College of Education for Pure Sciences, University of Mosul, Mosul, Iraq*
[2]*College of Health and Medical Techniques, Al-noor University, Mosul, Iraq*
[3]*Department of General Science, College of Basic Education, Salahaddin University, Erbil, Kurdistan region, Iraq*
email: mumtaz_hussien@alnoor.edu.iq;*abbas.rostam@su.edu.krd*
**Corresponding Author email: dr.ali1969@uomosul.edu.iq*
Received April 4, 2026; revised June 22, 2026; accepted June 30, 2026

We used the sp3s* tight-bonding method as a computational approach to calculate the energy band structure of AlAs crystals in the absence of pressure and analyzed the effect of pressure on the energy band structure under low pressure (1-7) GPa. We used two forms of the Birch-Maugham equation of state (third- and fourth-order) to calculate the changes in the elements of the Hamiltonian matrix resulting from changes in crystal volume and lattice constant. The dispersion relationships for the high-symmetry directions in the first Brillouin zone were found by numerically calculating the Hamiltonian diagonal under pressure. The present computations are performed using a routine written in MATLAB. We found that the effects of both forms of the equation of state on the band structure differ only slightly (by 0.01) at low pressure, as shown in the band structure diagrams. The conduction-band valleys creep downward under low pressure, decreasing both the direct and indirect energy gaps. The results obtained were consistent with other experimental and theoretical results.
Keywords: *Tight-bonding model; Maugham equation of state; AlAs compound semiconductor; Band structure; High pressure*

1. INTRODUCTION

Due to their great technological and industrial significance in the electronic applications and optoelectronic devices, III-V zinc-blende compound semiconductors have been widely regarded as the most promising compound semiconductors over the past few decades [1]. The study of materials at high pressures is currently experiencing great activity. The application of high pressure frequently leads to considerable shifts in both the chemical and physical properties of substances. Consequently, materials frequently exhibit previously unseen crystalline structures and intriguing behaviors when subjected to these conditions. Also, the possibility to study structural stability as a function of volume has added a fresh dimension to the basic question regarding the relation between the arrangement of atoms and electronic structure [2]. Particularly, Aluminum Arsenide (AlAs) is a binary compound that has an indirect band gap with the conduction band minimum at the X-point and the valence band maximum at the Γ-point under surrounding conditions. AlAs has an experimental band gap of about 2.16 eV [3]. The most stable phase for AlAs is the tetrahedral structure, a bonded semiconducting phase at ambient pressure, which has excellent physical properties, making it suitable for device applications such as optical fibers in telecommunication, Bragg reflector superlattices, heterojunction bipolar transistors, solid-state lasers, high electron mobility transistors, and light-emitting diodes [2], [3]. When moderate pressure is applied, like many other semiconductors, AlAs transforms into the metallic phase [4] [5]. Theoretical investigations and experimental research are therefore of vital interest to all those working in this area. In recent years, an increasing number of researchers have conducted experimental studies on the phase transition in AlAs. The first report of the phase transition of AlAs was made by Froyen and Cohen in 1983, who studied structural properties in AlAs using an ab initio pseudopotential approach and suggested that the case of high-pressure structure of AlAs commonly undergoes a structural transition, which could either be rock salt (B1) structure or NiAs (B8) structure [6]. Weinstein et al. observed a phase change by microscopic analysis at 12.3 GPa on loading; however, the structure was unidentified[7]. In subsequent years, an increasing number of researchers turned to experimental studies of the phase transition in AlAs. The first experimental observation of the transformation of AlAs into the NiAs structure came several years later, when G. Greene Raymond et al. indexed a new phase of AlAs using energy-dispersive X-ray diffraction to 46 GPa [8]. Mujica et al. offered a detailed review of the current known structures, high-pressure behavior, and theoretical work on the group III–V compound semiconductor materials [9]. Besides the experimental advance, dependable computational techniques designed for the determination of electronic band structures, as well as overall energy calculations, have significantly influenced the field of high-pressure physics [10], [11], [12]. These computational approaches yield critical supplemental data to that obtained through experimental investigation. This progress rises from both the development of amended algorithms and the increasing availability of powerful computing resources. Such theoretical work plays a supporting role to experimental research by both validating discovered structures and examining their electronic and vibrational features, as well as assisting in forecasting the shape of new materials.

This research aims to focus on theoretical calculations of the band structure and the effect of pressure on electronic properties, such as the band gap. Electronic property calculations are based on Harrison's model of semiconductors by

Cite as: A.A. Mohammed, M.M.S. Hussien, A.H. Rostam, East Eur. J. Phys. 3, 347 (2026), https://doi.org/10.26565/2312-4334-2026-3-30

constructing a nearest-neighbor semi-empirical tight-binding theory (TB). The effect of pressure at (1,3,5,7) GPa on the band gap energy of AlAs is investigated. The dependence of the energy states, over several symmetry directions and at certain symmetry points, on the interaction parameters is also investigated.

2. THEORETICAL BACKGROUND

2.1. Tight Binding Method

Electronic band structure is the energy range in which an electron is either forbidden or allowed to exist, and it's one of the important key to understanding electron conduct in crystalline semiconductors and their interactions with lattice vibrations[13]. One of the appealing method to calculate the electronic band structure of electron motion in solids is the tight binding theory (TB), which is called also linear combination of atomic orbitals (LCAO) proposed by Bloch [14]. The tight binding model is the standard technique for resolving issues related to periodic potentials. It entails constructing a linear combination of atomic orbitals $\phi_n(r-\vec{R}_i)$ on the various crystal atoms, with the coefficient given by the values of the plane wave $exp(i\vec{k}.\vec{R}_i)$ at the distinct vector positions $\vec{R}$,where the atoms are located, to form Bloch sum $\sum \vec{R}\, e^{(i\vec{k}.\vec{R}_i)}\phi_n(r-\vec{R}_i)$. The sum run over the atoms in equivalent position in all unit cells of the crystal, the subscript n denotes to quantum numbers [15]. In present work, the nearest neighbor sp^3s^* empirical tight binding method with fitted input parameters from the literature is used to calculate the band structure and energy gaps of the bulk compound semiconductor AlAs at some high symmetry points by preparing a computational program using MATLAB. The tight-binding model yields a detailed real space description of the electronic interactions that give rise specific elements of the energy band structure and density of states. This is very useful in research, where the electronic structure is modified and can see how these features convert when you change the electronic.

Although the tight-binding method is systematically inviting, it poses a major issue: the fundamental parameters that define the tight-binding Hamiltonian are not the conduction-band edges and effective masses typically employed in electronic-device modeling, but rather orbital interaction energies. The coupling of the separated orbitals via these interaction energies leads to the formation of electronic bands. A correct choice of the type and number of basic orbitals (s, p, and d) and of their local and non-local coupling strengths yields a suitable representation of material characteristics such as band energy structures and effective masses. Consequently, the overall band structure and effective masses are strongly linked to the interaction energies[16].

2.2. Calculation of Energy Band Structure

Quantum mechanics provides the only viable path for resolving numerous issues in physics and chemistry. In the case of zinc- blende crystals the, tight-binding Hamiltonian can be constructed in a basis of quasi-atomic functions as [17], [18]:

$$\left|n\lambda\vec{k}\right\rangle = \frac{1}{\sqrt{N}}\sum_{i,\lambda} \mathrm{e}^{(i\vec{k}.\vec{R}_i + i\vec{k}.\vec{v}_\lambda)}\left|n\lambda\vec{R}_i\right\rangle, \tag{1}$$

where $\vec{R}_i$ is the vector position of the atom on which the orbital is located, the quantum numbers (band index n) pass the s, p_x, p_y, p_z, and s^* orbitals; the number of unit cells in the repeating region is N where the wave vectors ($\vec{k} = 2\pi/a_l$) lie in the first Brillouin zone. The base atom displacement is indicated $\vec{v}_\lambda$ and in terms of Kronecker δ, we have $\vec{v}_\lambda = \delta_\lambda(a_l/2)(1,1,1)$; and λ =a (anion) or λ = c (cation) represents site index and the lattice constant represented by a_l.

In Bloch functions built from s and p orbitals (Wannier functions) located on each atom in the crystal, one assumes that the only non-zero Hamiltonian matrix elements are those between orbitals on the same or neighboring atoms [19]. This results in a relatively good description of the valence bands throughout the Brillouin zone. The sp^3s^* tight-binding method without spin-orbit coupling introduced by Vogl et al. (1983), which considers only nearest-neighbour interactions, uses Löwdin orbitals: an s-state and three p-states together with an excited s* state for each basis atom in pure bulk covalent semiconductors, providing ten orbitals for a primitive cell that contains two atoms.

The band structure for a nearest-neighbor, sp^3, eight- band model, is described by the nine parameters: four diagonal energies $E_{sa} = \langle sa\vec{R}|H|sa\vec{R}\rangle$, $E_{sc} = \langle sc\vec{R}|H|sc\vec{R}\rangle$, $E_{pa} = \langle p_x a\vec{R}|H|p_x a\vec{R}\rangle$ $E_{pc} = \langle p_x c\vec{R}|H|p_x c\vec{R}\rangle$ and the five transfer matrix elements V, $V_{ss} = 4\langle sa\vec{R}|H|sc\vec{R}\rangle$, $V_{xx} = 4\langle p_x a\vec{R}|H|p_x c\vec{R}\rangle$, $V_{xy} = 4\langle p_x a\vec{R}|H|p_y c\vec{R}\rangle$ $V_{sapc} = 4\langle sa\vec{R}|H|p_x c\vec{R}\rangle$ and $V_{pasc} = 4\langle p_x a\vec{R}|H|sc\vec{R}\rangle$.

In ten-band sp^3s^* model, besides these nine parameters, we add another an excited s state, s*, and allowing coupling only to the p states of neighbors, while excluding, for simplicity, the linkage to s-states on distant sites. This addition brings four additional matrix elements: specifically, two of these being new diagonal energies $E_{s^*a} = \langle s^* a\vec{R}|H|s^* a\vec{R}\rangle$, $E_{s^*c} = \langle s^* c\vec{R}|H|s^* c\vec{R}\rangle$, and the latter two being transfer matrix elements $V_{s^*apc} = 4\langle s^* a\vec{R}|H|p_x c\vec{R}\rangle$, $V_{pas^*c} = 4\langle p_x a\vec{R}|H|s^* c\vec{R}\rangle$. The following matrix elements which are being omitted for clarity, have been set to zero,: $\langle s^* a\vec{R}|H|s^* c\vec{R}\rangle$, $\langle s^* a\vec{R}|H|s\, c\vec{R}\rangle$and $\langle sa\vec{R}|H|s^* c\vec{R}\rangle$ [20].

By employing thirteen fitted input interaction parameters, derived from the theoretical data of Vogl's which are required to calculate the energy-band structure. These interaction parameters are essentially independent matrix elements, made up of: six on - site energies E_{sa} , E_{pa}, E_{sc} , E_{pc} , E_{s^*a} and E_{s^*c} (a, c refer to anion and cation

respectively) and seven hopping terms refer to V_{ss}, V_{xx}, V_{xy}, V_{sapc}, V_{pasc} , V_{s^*apc} and V_{pas^*c}. These matrix elements still need to be determined and fit for the band structure data; they can be provided in the Löwdin form of the symmetrically orthogonalized atomic orbitals. The input parameters representing the empirical matrix elements of the sp3s* tight binding model used to calculate band structure of the compound semiconductor AlAs are shown in Table (1).

For a zinc blende structure of lattice constant a, the wave vector (k) dependence in this tight binding model is given by defining the g_i coefficients [17],

$$\left.\begin{aligned} g_0(k) &= +cos\left(a_l\frac{k_1}{4}\right)cos\left(a_l\frac{k_2}{4}\right)cos\left(a_l\frac{k_3}{4}\right) - isin\left(a_l\frac{k_1}{4}\right)sin\left(a_l\frac{k_2}{4}\right)sin\left(a_l\frac{k_3}{4}\right) \\ g_1(k) &= -cos\left(a_l\frac{k_1}{4}\right)sin\left(a_l\frac{k_2}{4}\right)sin\left(a_l\frac{k_3}{4}\right) + isin\left(a_l\frac{k_1}{4}\right)cos\left(a_l\frac{k_2}{4}\right)cos\left(a_l\frac{k_3}{4}\right) \\ g_2(k) &= -sin\left(a_l\frac{k_1}{4}\right)cos\left(a_l\frac{k_2}{4}\right)sin\left(a_l\frac{k_3}{4}\right) + icos\left(a_l\frac{k_1}{4}\right)sin\left(a_l\frac{k_2}{4}\right)cos\left(a_l\frac{k_3}{4}\right) \\ g_3(k) &= -sin\left(a_l\frac{k_1}{4}\right)sin\left(a_l\frac{k_2}{4}\right)cos\left(a_l\frac{k_3}{4}\right) + icos\left(a_l\frac{k_1}{4}\right)cos\left(a_l\frac{k_2}{4}\right)sin\left(a_l\frac{k_3}{4}\right) \end{aligned}\right\} \quad (2)$$

Furthermore, the basic problem of the tight-binding method is to calculate the matrix elements of the Hamiltonian between the various basis states.

The secular equation for the eigenvalues E(k) and eigen functions is an 10×10 coupled set of equations, Hamiltonian matrix elements, whose solution is derived from an 10×10 secular equation. For each value of the wave vector (k), there will be 10 solutions, to obtain the band structure (E vs. k relationship) [17], [21].

Table 1. Tight binding method Input parameters for empirical matrix elements using sp3s*, all energies are in units of eV, for compound semiconductor AlAs at p=0 [17].

Parameters	AlAs with no pressure[17]
a_o	5.6580
E_{sa}	-7.5273
E_{pa}	0.9833
E_{sc}	-1.1627
E_{pc}	3.5867
E_{s^*a}	7.4833
E_{s^*c}	6.7267
V_{ss}	-6.6642
V_{xx}	1.8780
V_{xy}	4.2919
V_{sapc}	5.1106
V_{scpa}	5.4965
V_{s^*apc}	4.5216
V_{pas^*c}	4.9950

2.3. Calculation Energy Band Structure of AlAs Under Pressure

High pressures influence the physical characteristics of semiconductor materials and the physical systems in which they are contained. The energy band gaps E_g, where the electron direct (wave vector k is conserved) and indirect (k is non- conserved) transitions between the conduction band and valence band, together with their pressure dependence, are the subject of more studies as a fundamental property of semiconductor material [22], [23], [24]. To analyze the impact of pressure on the energy band structure, Murnaghan's equation of state can be used, which assumes that the bulk modulus of a solid under finite strain varies linearly with pressure. When hydrostatic pressure is applied to a crystal (typically as from 1-10 GPa), its lattice constant, length of unit cell edge, decreases, because the atoms are pushed closer together; then the entire size of the crystal decreases, which changes the periodicity of the crystal and cause to increases orbital overlap between neighboring atoms. The application of pressure can reduce the band gap or cause a transition from a direct to an indirect band gap [25].

The pressure dependence of the lattice parameter of AlAs is determined using the Murnaghan equation of state [26]:

$$a(p) = \mathrm{a}(0)\left(1 + B_o'\frac{p}{B_o}\right)^{\frac{-1}{3B_o}} \quad (3)$$

where $a(p)$ is the lattice parameter at pressure ($p \neq 0$), $\mathrm{a}(0)$ is the lattice constant at zero pressure ($p = 0$), and $B_o, B_o{}'$ are the isothermal bulk modulus and first derivative of the isothermal bulk modulus at zero and at pressure p respectively (in this work $\mathrm{B_o} = 76.2\ \mathrm{Gpa}, \mathrm{B_o}{}' = 4.36\ \mathrm{Gpa}$) [27]. A small decrease in the lattice constant causes a greater proportional decrease in the volume of the crystal unit cell because the volume is proportional to the cube of the

lattice constant for a cubic lattice (i.e. V = a³) [28]. A widely used Murnaghan equation of state (EOS) in terms of volume is:

$$V(p) = V(o)\left(1 + B_o' \frac{p}{B_o}\right)^{\frac{-1}{B_o}}, \tag{4}$$

where $V(p)$ and $V(o)$ are the volumes at pressure p and zero pressure respectively.

$$\frac{a(p)}{a(0)} = \left(\frac{V(p)}{V(0)}\right)^{\frac{1}{3}}. \tag{5}$$

The tight-binding matrix elements (hopping integrals) vary when pressure exerted since pressure decrease the interatomic distance between atoms in the crystal structure which reducing the bond lengths (d) and lattice constant. Due to this closeness, the overlap between atomic orbitals is enhanced, which raises the magnitude of tight-binding Hamiltonian matrix elements. In general, these matrix elements follow an power-law scaling with the interatomic distance in a way that stronger electronic coupling appears as atoms bring closer [29]. The change of energy band structure under pressure lead to change interatomic matrix elements for the coupling between s-states on neighboring atoms given by the empirical measurement rule [29], [30]:

$$V_{ll'm} = \eta_{ll'm} \frac{\hbar^2}{2m_e} d^{-2}. \tag{6}$$

$\eta_{ll'm}$ represents a universal dimensionless constant, $\hbar$ is the reduced Planck constant, and m_e is the mass of electron. Equation (6) can be expressed in the absence of pressure and in the presence of pressure on AlAs crystal, as follows:

$$V_{(0)} = \eta_{ll'm} \frac{\hbar^2}{2m_e} d_0^{-2}. \tag{7}$$

And

$$V_{(p)} = \eta_{ll'm} \frac{\hbar^2}{2m_e} d_p^{-2}. \tag{8}$$

Equations 5, 8, and 9 give a relationship that can be used to determine the energy band structure of AlAs by calculating the change in the matrix elements coefficients under pressure.

4. RESULTS AND DISCUSSION

4.1. Calculation Band structure at p= 0

We have applied the sp_3s^*empirical tight binding model to the energy band structure calculations for the bulk semiconductor compound of AlAs along the high symmetry axes in the Brillouin zone, and we are using a specially designed MATLAB. The band structure along the symmetry axes of L-Γ-X-U, K , is shown in Figure (1), where Γ is the Brillouin zone center; and X, L, K and U are the Brillouin zone edges for a zinc blende crystal of lattice constant a , used $a = 5.6580A^{\circ}$ for AlAs [17], [31]. The highest value of valence band maximum is placed at Γ while the lowest value of conduction minima is located at X.

Figure (1) shows the dispersion curves for bulk bands of AlAs for sp3s*, including valence bands and conduction bands. These band structures show certain features that are general to bulk semiconductors. It is seen from Figure (1) that AlAs is indirect band gaps with a minimum gap along X of semiconductor $E_{gX} = 2.3$ eV and direct extremum gap at Γ of $E_{g\Gamma} = 3.04$ eV. The results of calculating energy gap band at the high symmetry points L, Γ, and X at atmospheric pressure (p= 0), with respect to the first conduction band, were compared with the practical and theoretical results shown in Table (2).

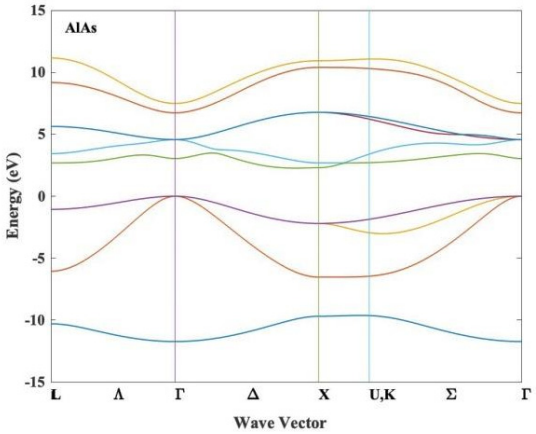

Figure 1. Energy band structure of AlAs obtained from sp^3s^* ETB model of AlAs.

Table 2. Energy band structure at high symmetry points at p= 0

Parameter	This work	Theoretical data [20]	Experimental data [32]
$E_{g\Gamma}$	3.0400	3.026	2.95
E_{gX}	2.3000	2.289	2.16
E_{gL}	2.6813	2.766	2.36

2. Calculation of band structure of AlAs at hydrostatic pressure

When the pressure is applied to an AlAs crystal, the lattice constant decreases, and therefore the volume reduces. In this study we used the Birch–Murnaghan EOS to compute the lattice constant under pressure, which then alter tight-binding parameters. This will change the energy bands structure. In this work, we compared between third and fourth order Birch-Maugham equation of state to compute the change in volume of the crystal. The fourth order Birch-Maugham equation of state (EOS_1) in which the pressure – volume relationship expanded as [33],[34]:

$$P = 3B_o f_e(1+2f_e)^{5/2}\left[1+\frac{3}{2}(B_o{}'-4)+\frac{3}{2}\left(B_oB_o{}''+(B_o{}'-4)(B_o{}'-3)+\frac{35}{9}\right)f_e{}^2\right] \quad (9)$$

where $f_e = \frac{1}{2}\left(((V/V_o)^{-2/3}-1\right)$ and the second derivative of $B_o$is given by [27]:

$$B_o{}'' = \frac{-1}{B_o}\left[(3-B_o{}')(4-B_o{}')+\frac{35}{9}\right] \quad (10)$$

The third order Birch-Maugham equation of state can be expressed by the following equation (EOS_2) is given by [35]:

$$P = \frac{3}{2}B_o\left[(x)^{7/3}-(x)^{5/3}\right]\left\{1+\frac{3}{4}[B_o{}'-4]\left[(x)^{2/3}-1\right]\right\} \quad (11)$$

where $x = V_o/V$, the second element within the first square bracket appears due to the truncation of the Helmholtz free energy to the third order term [36]. The 3rd and 4th Birch-Maugham forms give the relation between ratio of volume and pressure is shown in Figure (2).

From Fig. (2) the ratio V/V_o =1 when p=0, and it diminishes gradually at low pressure (under 10 GPa) indicates the unit cell volume becomes smaller. At low pressure the unit cell volume shrinks just a little (a few percent) and that means there is no influence when using both EOS_1 and EOS_2 forms to compute the effect of ratio V/V_o at low pressure range (the ratio almost less than 0.001) and the effect grows at high pressure (above 20 GPa). The EOS is the fundamental step that interprets applied pressure into lattice constant change, which then drives band structure modifications in tight-binding calculations. The ratio between the lattice constant under and lattice constant at p = 0 (a/a_o) for both two forms of equation of state versus pressure is shown in Figure (3). We noticed that the curve roughly linear at low pressures for both forms. The difference between Fig. (2) and Fig. (3) comes from the small reduction in lattice constant produces a large fractional reduction in volume since the lattice constant scales as one third of the volume of crystal (eq. (5)). Table three shows the values of the ratio for (V/V_o) , (a/a_o) versus pressure for both forms of EOS.

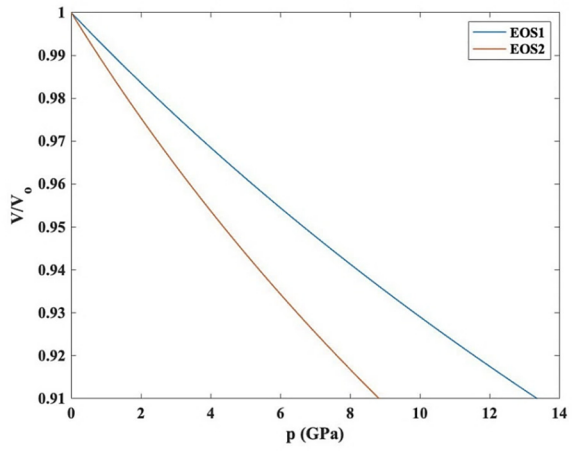

Figure 2. ratio of volume V/V_o versus pressure for both EOS_1 and EOS_2 forms

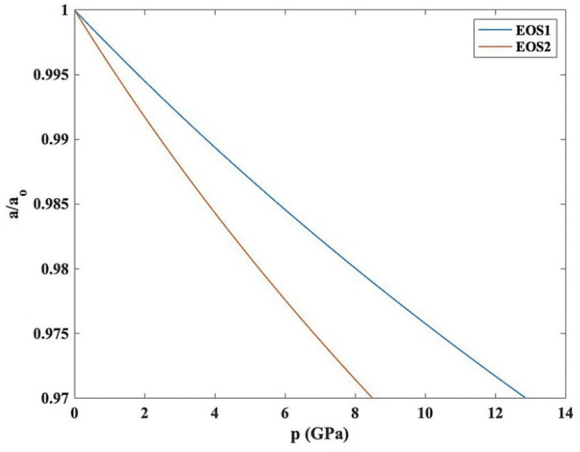

Figure 3. Ratio of lattice constant (a/a_o) versus pressure for both EOS_1 and EOS_2 forms

Table (3). Values of the ratio for V/V_o, (a/a_o) versus pressure for EOS_1 and EOS_2

Pressure (GPs)	EOS_1	EOS_2	EOS_1	EOS_2
	V/V_o	V/V_o	a/a_o	a/a_o
1	0.9917	0.9873	5.6422	5.6340
2	0.9836	0.9754	5.6270	5.6113
3	0.9759	0.9643	5.6123	5.5898
4	0.9685	0.9538	5.5980	5.5694
5	0.9614	0.9438	5.5842	5.5500
6	0.9545	0.9344	5.5708	5.5314
7	0.9478	0.9254	5.5578	5.5136
8	0.9414	0.9168	5.5452	5.4966
9	0.9351	0.9087	5.5329	5.4802
10	0.9291	0.9008	5.5210	5.4644

Employing both forms of EOS (Equations 9 and 11), we determined the volume and the lattice constant under pressure, where the orbital overlap and the hopping integral (matrix elements) in the ETB method are governed by the lattice constant. Using updated hopping integrals to build the Hamiltonian matrix element which consequently modifies the band structure for AlAs compound semiconductor.

The empirical tight-binding interaction parameters for both EOS_1 and EOS_2 forms are displayed in Table (4) and Table (5), respectively.

Table (4). The new empirical matrix elements of the sp^3s^* TB model in eV for AlAs at different values of pressure calculated from using EOS_1 , parameters of no pressure (p= 0) is fitted from the reference [17] .

Parameters	P = 0	P = 1 GPa	P = 3 GPa	P = 5 GPa	P = 7 GPa
E_{sa}	-7.5273	-7.4854	-7.4061	-7.3323	-7.2631
E_{pa}	0.9833	0.9778	0.9675	0.9578	0.9488
E_{sc}	-1.1627	-1.1562	-1.1440	-1.1326	-1.1219
E_{pc}	3.5867	3.5667	3.5289	3.4938	3.4608
E_{s^*a}	7.4833	7.4416	7.3628	7.2894	7.2207
E_{s^*c}	6.7267	6.6892	6.6184	6.5524	6.4906
V_{ss}	-6.6642	-6.6271	-6.5569	-6.4915	-6.4303
V_{xx}	1.8780	1.8675	1.8478	1.8293	1.8121
V_{xy}	4.2919	4.2680	4.2228	4.1807	4.1413
V_{sapc}	5.1106	5.0821	5.0283	4.9782	4.9313
V_{scpa}	5.4965	5.4659	5.4080	5.3541	5.3036
V_{s^*apc}	4.5216	4.4964	4.4488	4.4044	4.3629
V_{pas^*c}	4.9950	4.9672	4.9146	4.8656	4.8197

Table (5). The new empirical matrix elements of the sp^3s^* TB model in eV for AlAs at different values of pressure calculated from using EOS_2

Parameters	P = 0 [17]	P = 1 GPa	P = 3 GPa	P = 5 GPa	P = 7 GPa
E_{sa}	-7.5273	-7.4635	-7.3470	-7.2426	-7.1480
E_{pa}	0.9833	0.9750	0.9597	0.9461	0.9338
E_{sc}	-1.1627	-1.1528	-1.1349	-1.1187	-1.1041
E_{pc}	3.5867	3.5563	3.5008	3.4510	3.4060
E_{s^*a}	7.4833	7.4199	7.3041	7.2003	7.1063
E_{s^*c}	6.7267	6.6697	6.5656	6.4723	6.3878
V_{ss}	-6.6642	-6.6077	-6.5046	-6.4122	-6.3284
V_{xx}	1.8780	1.8621	1.8330	1.8070	1.7834
V_{xy}	4.2919	4.2555	4.1891	4.1296	4.0757
V_{sapc}	5.1106	5.0673	4.9882	4.9173	4.8531
V_{scpa}	5.4965	5.4499	5.3648	5.2886	5.2196
V_{s^*apc}	4.5216	4.4833	4.4133	4.3506	4.2938
V_{pas^*c}	4.9950	4.9527	4.8754	4.8061	4.7433

The energy band structures for both EOS_1 and EOS_2 forms of Birch-Maugham equation of state under pressure after determining the change in matrix elements are shown in Fig. (4) and Fig (5). We see from figures the change in band structure is less than 0.01 (< 0.01) using both EOS forms and the energy gap smoothly reduced

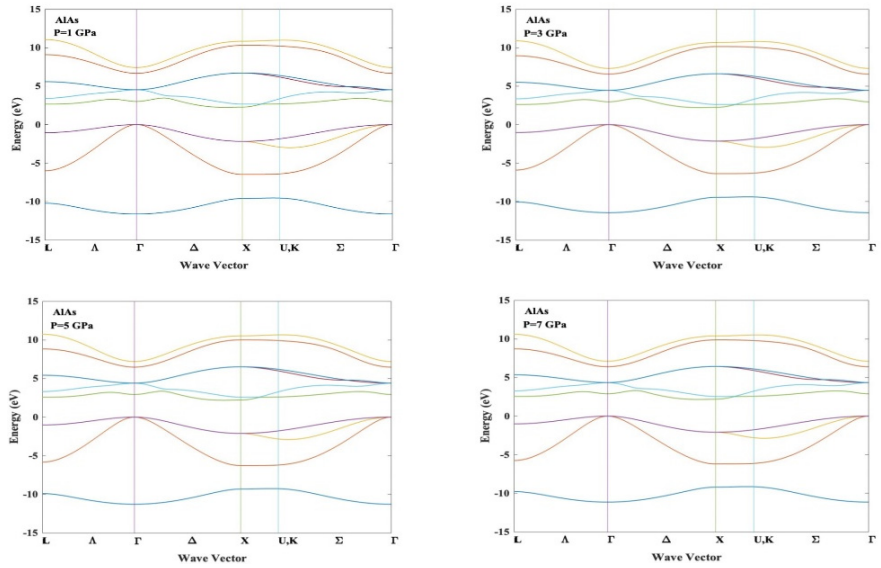

Figure 4. Energy band structure obtained from sp^3s^* ETB model of AlAs under pressures (1,3,5,7) GPa applying 4th order Birch-Maugham equation of state

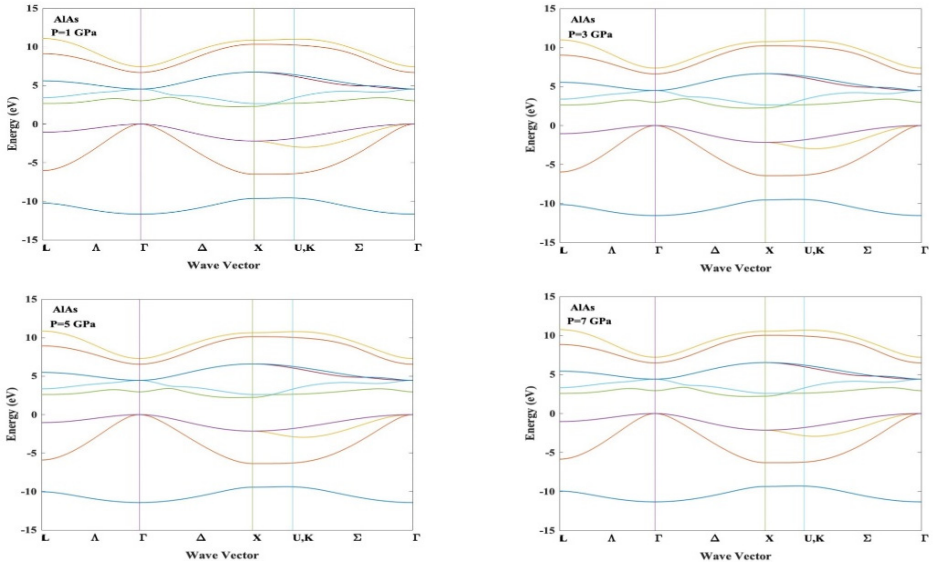

Figure 5. Energy band structure obtained from sp^3s^* ETB model of AlAs under pressures (1,3,5,7) GPa applying 3rd order Birch-Maugham equation of state

From the figures, we observe similar results appear at low pressures, in the range (1-7) GPa, for both forms of the equation of state, and we notice that AlAs has an indirect band gap at $\Gamma \rightarrow X$ and direct band gap at $\Gamma \rightarrow \Gamma$. We expect that the energy gaps roughly decrease linearly since the X conduction band edge decreases more rapidly than the rise of the valence band edge. The energy band gaps at high symmetry points using two forms of equation of state are displayed in Table (6) and shown in Figure (6).

Table (6). The energy gap of AlAs with low pressure for the high symmetry points Γ, L, X using two equations of states

P (GPa)	EOS 1			EOS 2		
	$E_{g\Gamma}$	E_{gL}	E_{gX}	$E_{g\Gamma}$	E_{gL}	E_{gX}
0	3.0400	2.6813	2.3000	3.0400	2.6813	2.3000
1	3.0231	2.6663	2.2872	3.0143	2.6586	2.2805
3	2.9911	2.6381	2.2630	2.9672	2.6170	2.2450
5	2.9612	2.6118	2.2405	2.9251	2.5799	2.2130
7	2.9333	2.5872	2.2193	2.8869	2.5462	2.1841

As pressure increases, the conduction valleys shift downward while the maximum valence bands shift upward slightly, thereby decreasing the band gap [37]. From Figure (6) we observed that at low pressures (1,2,3) GPa curves for both EOS forms produce somewhat different pressure curves and the different between them nearly equal 0.07 at 7 GPa (~ 0.07). We note that the EOS_1 exhibit a bend in almost higher band gap values at same pressure since it takes into

account higher order elastic influences, but the difference is tiny at low pressures that is the reason the curve of EOS_1 is positioned over EOS_2 curve.

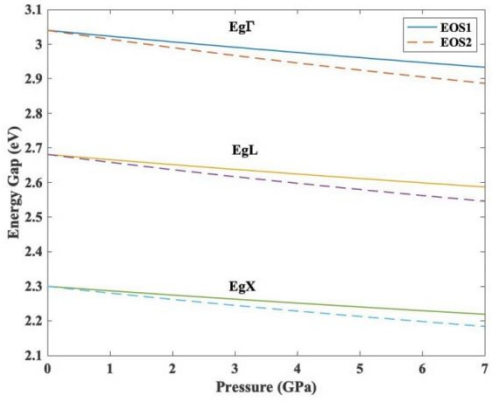

Figure 6. Energy band structure of AlAs under pressures (1,3,5,7) GPa at high symmetry points using both EOS forms

Table (7). The variation of E_g with pressure for direct and indirect for both EOS forms

P(GPa)	EOS_1		EOS_2	
	Eg (eV) Direct	Eg (eV) Indirect	Eg (eV) Direct	Eg (eV) Indirect
0	3.0400	2.2680	3.0400	2.2680
1	3.0231	2.2553	3.0143	2.2487
3	2.9911	2.2314	2.9672	2.2136
5	2.9612	2.2092	2.9251	2.1822
7	2.9333	2.1884	2.8869	2.1537

Table (7) shows the change in the direct and indirect band gap with pressure for both equation of state (EOS) forms of AlAs at low pressure. The variation of the direct and indirect band gap for both EOS forms is shown in Figure (7).

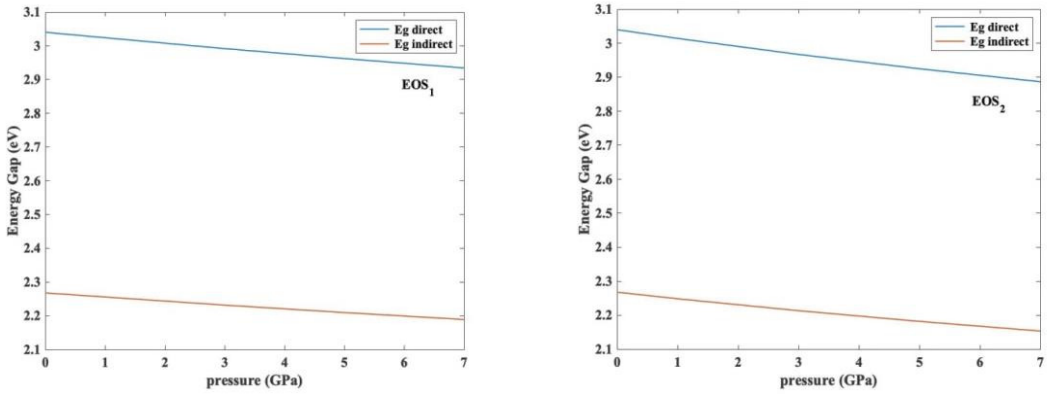

Figure 7. Direct and indirect energy gap with pressure for both EOS forms

The relationship between the conduction band and the wave vector at different low pressures is shown in Figure (8). It can be observed that with increasing pressure, the conduction bands creep downwards, and it can also be observed that the difference is very small when using the two equations of state formulas.

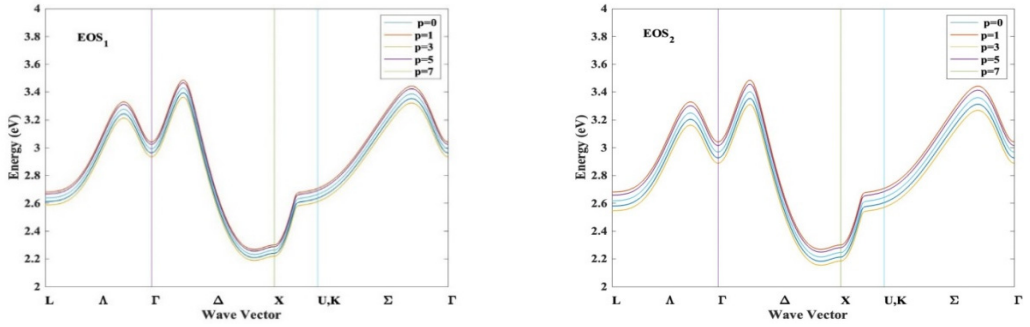

Figure 8. Comparison of the conduction band structure of AlAs without pressure and with pressures (1,3,5,7) GPa at high symmetry points using both EOS forms.

5. CONCLUSIONS

In this work, we found that in the absence of pressure, AlAs has an indirect band gap along X ($E_{gX} = 2.3$ eV) and a maximum direct energy gap at Γ of ($E_{g\Gamma} = 3.04$ eV), where the band-gap calculation is performed at high-symmetry points. We used two forms of the Birch-Murnaghan equation of state (4th and 3rd EOS) to determine the new empirical matrix elements, which are used to calculate the energy band structure under pressure. The change in band structure is less than 0.01 (< 0.01) by using both EOS forms, and the energy gap is smoothly reduced linearly with low pressure in the range 1-7 GPa. At low pressures (1,2,3) GPa curves for both EOS forms produce somewhat different pressure band structure curves, and the difference between them is nearly equal 0.07 at 7 GPa (~ 0.07). We note that the 4th order EOS_1 exhibits a bend in almost higher band gap values at the same pressure since it takes into account higher order elastic influences, but the difference is still tiny at low pressures that is the reason the curve of EOS_1 is positioned over EOS_2 curve. Finally, we expect that the high order of EOS is used at moderate (up to 20-30 GPa) and high pressure (up to 50 GPa), and the choice between third and fourth orders in the tight-binding model depends on whether we need qualitative or quantitative fineness under high pressure.

ORCID

Ali A. Mohammed, https://orcid.org/0000-0002-1731-3391; **Mumtaz M.S. Hussien,** https://orcid.org/0000-0002-4350-9523
Abbas Hussein Rostam, https://orcid.org/0009-0002-1852-4032

REFERENCES

[1] A. Srivastava, and N. Tyagi, "High pressure behavior of AlAs nanocrystals: the first-principle study," High Pressure Research, **32**(1), 43–47 (2012), https://doi.org/10.1080/08957959.2011.643791
[2] N. Y. Aouina, F. Mezrag, M. Boucenna, M. El-Farra, and N. Bouarissa, "High pressure electronic properties and elastic stability criteria of AlAs," Materials Science and Engineering: B, **123**(1), 87–93 (20050. https://doi.org/10.1016/j.mseb.2005.07.008
[3] F. Betraoui, H. Rekab- Djabri, K. Baddari, and S. Daoud, "Study of the Phase Transition and Physical Properties of AlAs, ScAs and Al_x Sc_{1-x} As Compounds by the FP-LMTO Method," Annals of West University of Timisoara - Physics, **66**(1), 118–141 (2024). https://doi.org/10.2478/awutp-2024-0008
[4] M. S. Ali and R. Parvin, "Investigation of pressure effect on structural, mechanical, electrical and optical properties of AlAs for optoelectronic applications," Physica B: Condensed Matter, **673**, 415491 (2024). https://doi.org/10.1016/j.physb.2023.415491
[5] V. B. Sheeba and C. N. Louis, "Band Structure, Metallization and Superconducting Transition Of Group III-V Semiconductors AlP And AlAs Under High Pressure," CME, **1**(4), 132–140 (2013). https://doi.org/10.13189/cme.2013.010405
[6] S. Froyen and M. L. Cohen, "Structural properties of III-V zinc-blende semiconductors under pressure," Phys. Rev. B, **28**(6), 3258–3265 (1983). https://doi.org/10.1103/PhysRevB.28.3258
[7] B. A. Weinstein, and S. K. Hark, "Phase Transitions in AlAs/GaAs Superlattices under High Pressure," Physical Review Letters, **58** (1987). https://doi.org/10.1103/physrevlett.58.781
[8] R. G. Greene, H. Luo, T. Li, and A. L. Ruoff, "Phase transformation of AlAs to NiAs structure at high pressure," Phys. Rev. Lett., **72**(13), 2045–2048 (1994). https://doi.org/10.1103/PhysRevLett.72.2045
[10] S. Adachi, "Band gaps and refractive indices of AlGaAsSb, GaInAsSb, and InPAsSb: Key properties for a variety of the 2–4-μm optoelectronic device applications," Journal of Applied Physics, **61**(10), 4869–4876 (1987). https://doi.org/10.1063/1.338352
[11] N. Bouarissa, "Electronic structure and lattice properties of zinc-blende InN under high pressure," The European Physical Journal B - Condensed Matter, **26**(2), 153–158 (2002). https://doi.org/10.1140/epjb/e20020076
[12] R. G. Greene, H. Luo, K. Ghandehari, and A. L. Ruoff, "High pressure structural study of AlSb to 50 GPa," Journal of Physics and Chemistry of Solids, **56**(3–4), 517–520 (1995). https://doi.org/10.1016/0022-3697(94)00231-2
[13] Adnan Al-sheikh, Mumtaz Hussien, and Siham Abdullah, "Pressure and Temperature Dependence of Energy Gap in SiC and Si1-xGex," RJS, **28**(4), 53–61 (2019). https://doi.org/10.33899/rjs.2019.163296
[14] T. B. Boykin, "Incorporation of incompleteness in the **k** · **p** perturbation theory," Phys. Rev. B, **52**(23), 16317–16320 (1995). https://doi.org/10.1103/PhysRevB.52.16317
[15] J. C. Slater and G. F. Koster, "Simplified LCAO Method for the Periodic Potential Problem," Phys. Rev. **94**(6), 1498–1524 (1954). https://doi.org/10.1103/PhysRev.94.1498
[16] Gerhard Klimeck, R. Chris Bowen, Timothy B. Boykin, Carlos Salazar-Lazaro, Thomas A. Cwik, and Adrian Stoica, "Si Tight-Binding Parameters from Genetic Algorithm Fitting," Superlattices and Microstructures, **27**(2/3), (2000). https://doi.org/10.1006/spmi.1999.0797
[17] P. Vogl, H. P. Hjalmarson, and J. D. Dow, "A Semi-empirical tight-binding theory of the electronic structure of semiconductors†," Journal of Physics and Chemistry of Solids, **44**(5), 365–378 (1983). https://doi.org/10.1016/0022-3697(83)90064-1
[18] D. A. Rasero Causil, A. A. Portacio, and D. Suescun, "Estructura Electrónica de GaAs y AlAs usando un Hamiltoniano Tight-Binding sp3s∗," Cienc. En Desarro, **12**(2), (2021). https://doi.org/10.19053/01217488.v12.n2.2021.12612
[19] D. J. Chadi, "Spin-orbit splitting in crystalline and compositionally disordered semiconductors," Phys. Rev. B, **16**(2), 790–796 (1977). https://doi.org/10.1103/PhysRevB.16.790
[20] G. Gopir, N. D. Zulkifli, and A. P. Othman, "Electronic Structure Calculation of Bulk Semiconductors Using The Sp3s* Empirical Tight Binding Method," Solid State Science and Technology, **13**(1), (2005).
[21] J. Singh, *Electronic and Optoelectronic Properties of Semiconductor Structures*, (First. Cambridge University Press, New York, 2003).
[22] A. A. Kelsey, and G. J. Ackland, "Computational analysis of the high-pressure structures of InSb," J. Phys.: Condens. Matter, **12**(32), 7161–7173 (2000). https://doi.org/10.1088/0953-8984/12/32/301

[23] Y. Ida, Y. Syono, and S. Akimoto, "Effect of Pressure on the Lattice Parameters of Stishovite," Earth and Planetary Science Letters, **3**, 216–218 (1968). https://doi.org/10.1016/0012-821X(67)90040-4
[24] M. S. Ali and R. Parvin, "Investigation of pressure effect on structural, mechanical, electrical and optical properties of AlAs for optoelectronic applications," Physica B: Condensed Matter, **673**, 415491 (2024). https://doi.org/10.1016/j.physb.2023.415491
[25] E. B. Elkenany, O. A. Alfrnwani, and M. Sallah, "Insight into pressure effect on optoelectronic, mechanical, and lattice vibrational properties of nanostructured $Ga_xIn_{1-x}P_ySb_zAs_{1-y-z}$ for the solar cells system," Sci. Rep. **13**(1), 3891 (2023). https://doi.org/10.1038/s41598-023-30681-1
[26] I. O. Radi, M. A. Abdulsattar, and A. M. Abdul-Lettif, "Semiempirical LUC-INDO calculations on the effect of pressure on the electronic structure of diamond," Physica Status Solidi (b), **244**(4), 1304–1317 (2007). https://doi.org/10.1002/pssb.200541329
[27] H.-Y. Wang, X.-S. Li, C.-Y. Li, and K.-F. Wang, "First-principles study of phase transition and structural properties of AlAs," Materials Chemistry and Physics, **117**(2–3), 373–376 (2009). https://doi.org/10.1016/j.matchemphys.2009.06.006
[28] V. G. Tyuterev, and N. Vast, "Murnaghan's equation of state for the electronic ground state energy," Computational Materials Science, **38**(2), 350–353 (2006). https://doi.org/10.1016/j.commatsci.2005.08.012
[29] S. Froyen and W. A. Harrison, "Elementary prediction of linear combination of atomic orbitals matrix elements," Phys. Rev. B, **20**(6), 2420–2422 (1979). https://doi.org/10.1103/PhysRevB.20.2420
[30] W. A. Harrison, "Elementary theory of heterojunctions," Journal of Vacuum Science and Technology, **14**(4), 1016–1021 (1977). https://doi.org/10.1116/1.569312
[31] I. Vurgaftman, J. R. Meyer, and L. R. Ram-Mohan, "Band parameters for III–V compound semiconductors and their alloys," Journal of Applied Physics, **89**(11), 5815–5875 (2001). https://doi.org/10.1063/1.1368156
[32] S. Adachi, "Band gaps and refractive indices of AlGaAsSb, GaInAsSb, and InPAsSb: Key properties for a variety of the 2–4-μm optoelectronic device applications," Journal of Applied Physics, **61**(10), 4869–4876 (1987). https://doi.org/10.1063/1.338352
[33] F. Birch, "Finite Elastic Strain of Cubic Crystals," Phys. Rev. **71**(11), 809–824 (1947). https://doi.org/10.1103/PhysRev.71.809
[34] T. Katsura, and Y. Tange, "A Simple Derivation of the Birch–Murnaghan Equations of State (EOSs) and Comparison with EOSs Derived from Other Definitions of Finite Strain," Minerals, **9**(12), 745 (2019). https://doi.org/10.3390/min9120745
[35] A. Al-sheikh, M. Hussien, and S. Abdullah, "Pressure and Temperature Dependence of Energy Gap in SiC and $Si_{1-x}Ge_x$," RJS, **28**(4), 53–61 (2019). https://doi.org/10.33899/rjs.2019.163296
[36] A. B. Alchagirov, J. P. Perdew, J. C. Boettger, R. C. Albers, and C. Fiolhais, "Energy and pressure versus volume: Equations of state motivated by the stabilized jellium model," Phys. Rev. B, **63**(22), 224115 (2001). https://doi.org/10.1103/PhysRevB.63.224115
[37] S. F. Mohammed, S. M. A. Ridha, A. M. Ghaleb, Z. T. Ghaleb, Y. Benkrima, and M. A. Abdullah, "Determination of Band Structure and Compton profiles for Aluminum-Arsenide Using Density Functional Theory," East Eur. J. Phys. (2), 132–137 (2023). https://doi.org/10.26565/2312-4334-2023-2-12

ВПЛИВ ТИСКУ НА ЕНЕРГЕТИЧНУ ЗОННУ СТРУКТУРУ AlAs ЗА ВИКОРИСТАННЯ МОДЕЛІ sp3s*

Алі А. Мохаммед[1], Мумтаз М.С. Хуссієн[2], Аббас Хуссейн Ростам[3]
[1]Кафедра фізики, Коледж освіти чистих наук, Університет Мосула, Мосул, Ірак
[2]Коледж охорони здоров'я та медичної техніки, Університет Аль-Нур, Мосул, Ірак
[3]Кафедра загальних наук, Коледж базової освіти, Університет Салахадділа, Ербіль, регіон Курдистан, Ірак

Ми використали метод щільного зв'язку sp3s* як обчислювальний підхід для розрахунку зонної структури кристалів AlAs за відсутності тиску та проаналізували вплив тиску на зонну структуру за низького тиску (1-7) ГПа. Ми використали дві форми рівняння стану Бірча-Моема (третього та четвертого порядку) для розрахунку змін елементів матриці Гамільтона, що виникають внаслідок змін об'єму кристалу та постійної решітки. Дисперсійні співвідношення для напрямків високої симетрії в першій зоні Бріллюена були знайдені шляхом чисельного розрахунку діагоналі Гамільтона під тиском. Ці розрахунки виконані за допомогою процедури, написаної в MATLAB. Ми виявили, що вплив обох форм рівняння стану на зонну структуру відрізняється лише незначно (на 0,01) за низького тиску, як показано на діаграмах зонної структури. Долини зони провідності спускаються вниз за низького тиску, зменшуючи як прямі, так і непрямі енергетичні щілини. Отримані результати узгоджуються з іншими експериментальними та теоретичними даними.

Ключові слова: *модель щільного зв'язку; рівняння стану Моема; складний напівпровідник AlAs; зонна структура; високий тиск*